Cell Chemical Biology, Volume *23*

Supplemental Information

Bidirectional Allosteric Communication between the ATP-Binding Site and the Regulatory PIF Pocket in PDK1 Protein Kinase

Jörg O. Schulze, Giorgio Saladino, Katrien Busschots, Sonja Neimanis, Evelyn Süß, Dalibor Odadzic, Stefan Zeuzem, Valerie Hindie, Amanda K. Herbrand, María-Natalia Lisa, Pedro M. Alzari, Francesco L. Gervasio, and Ricardo M. Biondi

Supplemental Information

Bidirectional allosteric communication between the ATP-binding site and the regulatory PIF-pocket in PDK1 protein kinase

Jörg O. Schulze[1]†, Giorgio Saladino[2]†, Katrien Busschots[1]‡, Sonja Neimanis[1]‡, Evelyn Süß[1], Dalibor Odadzic[1], Stefan Zeuzem[1], Valerie Hindie[1]‡, Amanda K. Herbrand[1], María-Natalia Lisa[3], Pedro M. Alzari[3], Francesco L. Gervasio[2,4]* and Ricardo M. Biondi[1,5]* ⁑

[1]Research Group PhosphoSites, Department of Internal Medicine I, Universitätsklinikum Frankfurt, Theodor-Stern-Kai 7, 60590 Frankfurt; [2]Department of Chemistry, University College London, 20 Gordon Street London WC1H 0AJ, UK; [3]Structural Biochemistry Unit, Pasteur Institute, Rue du Dr. Roux 25, F-75724 Paris, France; [4]Research Department of Structural and Molecular Biology, University College London, Gower Street, London WC1E 6BT, UK; [5]German Cancer Consortium (DKTK), Heidelberg, Germany; German Cancer Research Center (DKFZ), Heidelberg, Germany.

†Jörg O. Schulze and Giorgio Saladino contributed equally to this work

‡ Present addresses: K.B., European Commission, DG Joint Research Centre, Directorate F - Health, Consumer and Reference Materials, Geel, Belgium. V.H., Hybrigenics services, Paris, France. S.N., Klinik für Kinder- und Jugendmedizin, Universitätsklinikum Frankfurt, Frankfurt, Germany. M.N.L., Laboratory of Molecular & Structural Microbiology, Institut Pasteur de Montevideo, Mataojo 2020, Montevideo, 11400, Uruguay. R.M.B., additional current address, Instituto de Investigación en Biomedicina de Buenos Aires (IBioBA) - CONICET - Partner Institute of the Max Planck Society, Buenos Aires C1425FQD, Argentina

*Corresponding authors: R.M.B. (e-mail: biondi@med.uni-frankfurt.de) and F.L.G. (e-mail: f.l.gervasio@ucl.ac.uk)

⁑ Lead Contact: R.M.B.

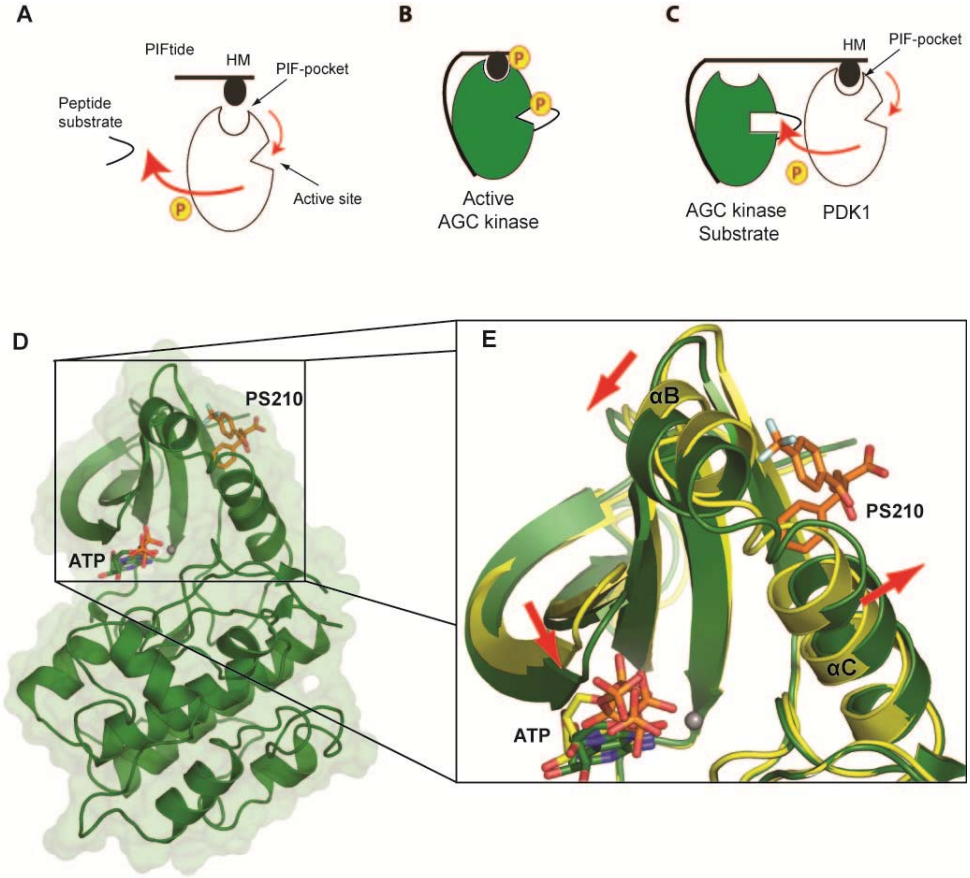

Figure S1. Related to Figure 1. Role of the PIF-pocket in the activation of AGC kinases and in the docking interaction of PDK1 with substrates. (**A**) Scheme of the catalytic domain of an AGC kinase that is activated in trans by a polypeptide comprising a hydrophobic motif (HM), such as PIFtide. The scheme represents the PDK1 *in vitro* activity assay used in this work (Biondi, et al., 2000). The mechanism of activation of by the binding of HM to the PIF-pocket has also been described in members of multiple families of kinases within the AGC kinase group, such as SGK, S6K, RSK, MSK, PKC (Biondi, et al., 2001; Frodin, et al., 2002) and Akt/PKB (Biondi, et al., 2001; Frodin, et al., 2002; Yang, et al., 2002). (**B**) Scheme representing a prototype AGC kinase. The HM, which is located C-terminal to the catalytic domain, binds intramolecularly to the PIF-pocket and acts in concert with the activation loop to stabilize the active conformation after HM and activation loop phosphorylation. (**C**) The PIF-pocket of PDK1 is the docking site for the specific docking interaction with substrates. PDK1 is a conformational sensor that only interacts with inactive protein kinases, which are recognized by the exposure of the HM. The docking interaction between the HM sequence and the PIF-pocket provides selectivity for the phosphorylation of substrates and also activates PDK1. The docking interaction is required for the phosphorylation of most substrates of PDK1 studied (e.g. S6K, SGK, PKCs, PRKs), but not for the phosphorylation of Akt/PKB, as verified *in vitro* (Biondi, et al., 2001) and in cells in culture (Bayascas, 2008; Collins, et al., 2003). Upon activation loop phosphorylation, the substrate acquires the active conformation as shown in (B). While PKA is an AGC kinase, its catalytic domain has evolved to be regulated by the interacting subunit and not by the PIF-pocket. In PKA, the C-terminal HM is constitutively docked into the PIF-pocket and does not play a regulatory role as described for other members of the AGC kinase group. (**D**) Allosteric activation of PDK1 by small compounds binding to the PIF-pocket. The binding of small compounds to the PIF-pocket produces local changes at the binding site and also allosteric effects at the activation loop and the Gly-rich loop, as verified in crystallography and deuterium exchange experiments (Hindie, et al., 2009). The allosteric effect on the ATP-binding site was confirmed using a fluorescent ATP probe, whose florescence varied in the presence of activating compounds that bind to the PIF-pocket (Hindie, et al., 2009). The allosteric effect on the ATP-binding site was most notably observed in the crystal structure of PDK1 in complex with PS210. The binding of PS210 induces the complete closure of the ATP-binding site, similar to the most closed-active structure of PKA(Zheng, et al., 1993).

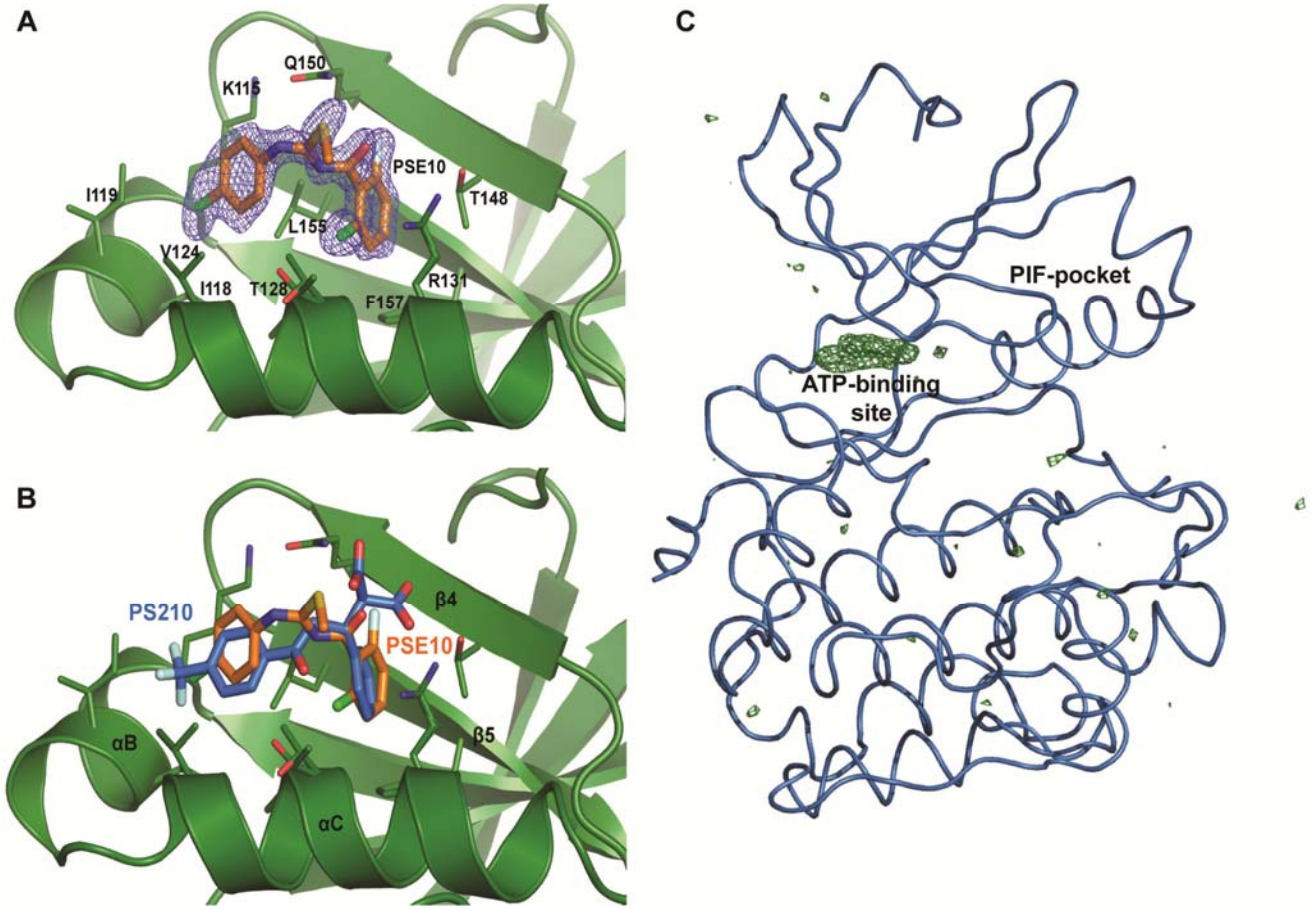

Figure S2. Related to Figure 1, Figure 2 and Table S1. Crystal structure of PDK1 in complex with PSE10 in comparison to PS210. **(A)** PDK1 (green) is shown in cartoon representation with residues in direct contact with allosteric compound PSE10 (orange carbon atoms) shown as sticks. $|2F_o\text{-}F_c|$ electron density of the compound is shown in blue and contoured at 1σ. **(B)** Superposition with the crystal structure of PS210 (blue carbon atoms) bound to PDK1 (PDB ID 4AW1). The binding mode of both compounds is very similar. The two ring systems align well and occupy the same subpockets of the PIF-pocket. (**C**) PS653 binds only to the ATP-binding site. $|F_o\text{-}F_c|$ electron density of the whole structure is shown in green and contoured at 5σ. This "positive difference density" represents only electron density that is not explained well by the structural model. For comparison, PS653 was omitted from the structure before calculation. No electron density of a second PS653 molecule can be observed, in particular not in the PIF-pocket. The remaining difference density belongs only to lowly occupied alternative water molecules and side chains.

A

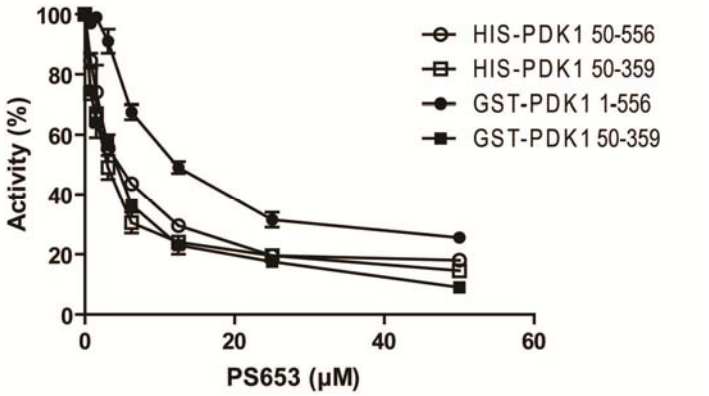

B

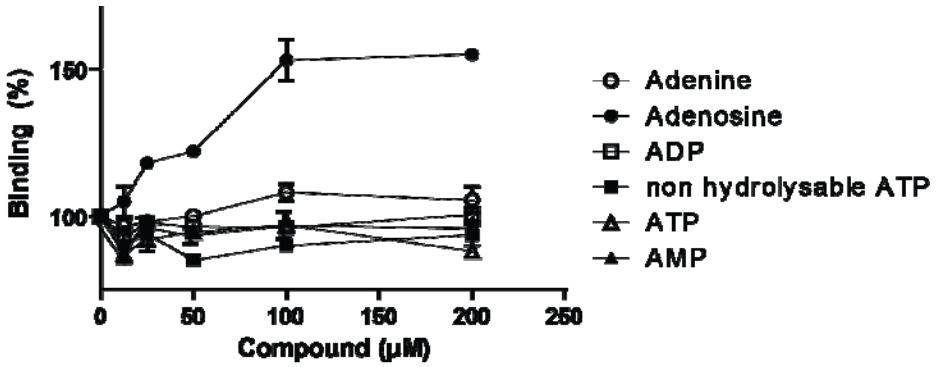

Figure S3. Related to Figures 1 and 2. Effect of small compounds that bind at the ATP-binding site on the allosteric modulation of the interaction with PIFtide. **A.** Effect of PS653 negative allosteric modulator on the *in vitro* activity of PDK1. PS653 inhibits the activity of His-PDK1, GST-PDK1, His-PDK1$_{50-359}$ and GST-PDK1$_{1-359}$. PDK1 comprises a catalytic domain located N-terminally and a C-terminal PH domain. PS653 inhibits the activity of different constructs of PDK1 comprising or lacking the first 49 aminoacids or the C-terminal region comprising the PH domain (His-PDK1 1-556, IC50= 3,3 μM, IC= 1,5-7,3 μM; GST-PDK1 1-556, IC50= 7,9 μM, IC= 6,3-9,9 μM; His-PDK1$_{50-359}$ [Tyr288Gly; Gln292Ala], IC50= 3,3, IC= 2,3-4,4 μM and GST-PDK1$_{1-359}$ [Tyr288Gly; Gln292Ala], IC50= 5,1 μM; CI= 3,6-7,2 μM). CI, 95% confidence interval. **B.** Adenosine is a positive allosteric modulator that binds to the ATP-binding site of PDK1 and enhances the interaction with PIFtide. The interaction was measured using the alphascreen assay described in Figure 1. Adenine, AMP, ADP, ATP or the non-hydrolizable ATP analog (up to 200 μM), do not affect the interaction of PDK1 with PIFtide.

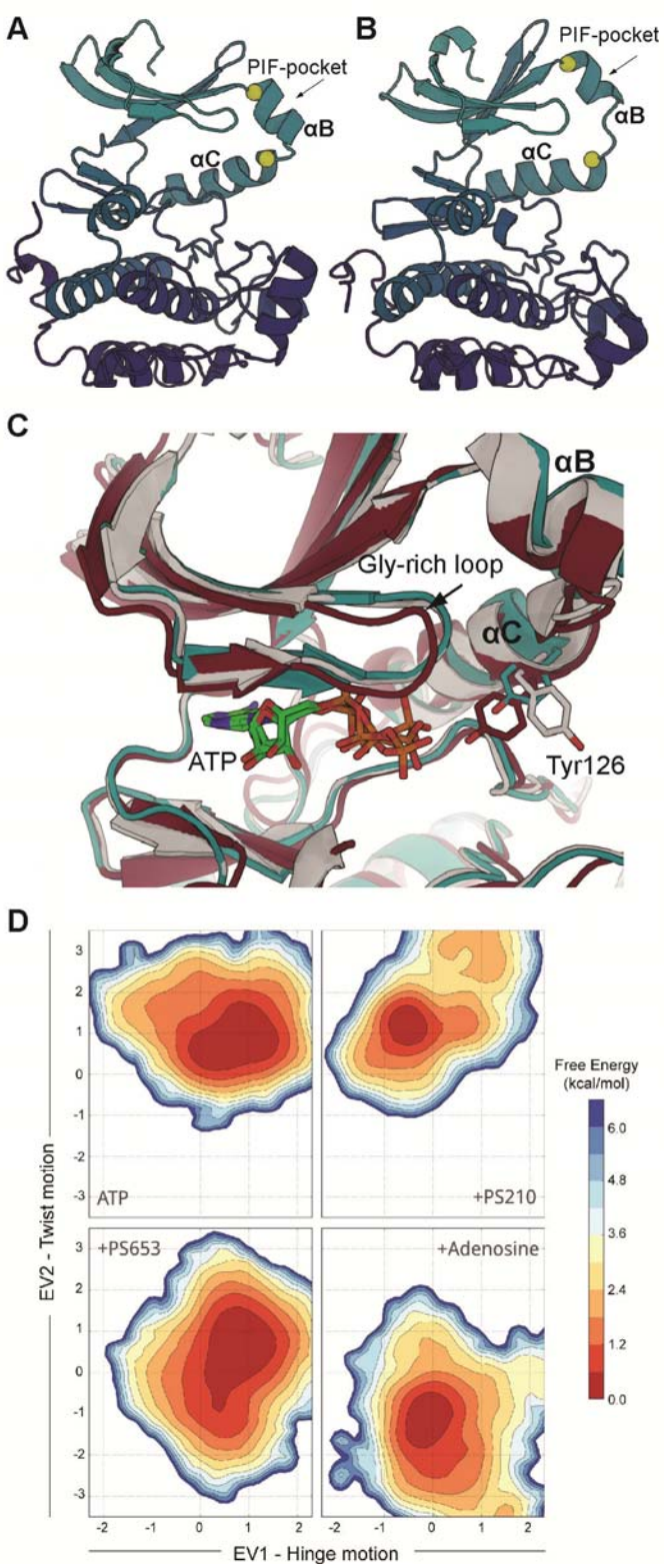

Figure S4. Related to Figure 3. Structure of PDK1 from the 400ns MD simulation. (**A-B**) Two different conformations are observed (a-b) differing by the orientation of helix αB. The residues used to compute the end-to-end distance (later in the main text) are highlighted as yellow spheres. (**C**) Different orientations of Tyr126 from the simulation (gray, main orientation; cyan, alternative orientation) and from the new crystal (purple). (**D**) Projection of the free energy along the first two PCA vectors obtained from the unbiased MD of PDK1 with ATP. When PS210 is bound, the accessible conformations span a narrower range of values along both the first eigenvector, which describes the *hinge motion*, and the second, which depicts the rotation ("twist") of the N-lobe with respect to the C-lobe. Interestingly, the twist movement coincides with the opening of the ATP-binding site, and its suppression upon PS210 binding also leads to tighter binding. This is in perfect agreement with the crystal structure of PDK1 in complex with PS210, which shows a rotation of the hinge resulting in the most closed structure of PDK1(Busschots, et al., 2012).

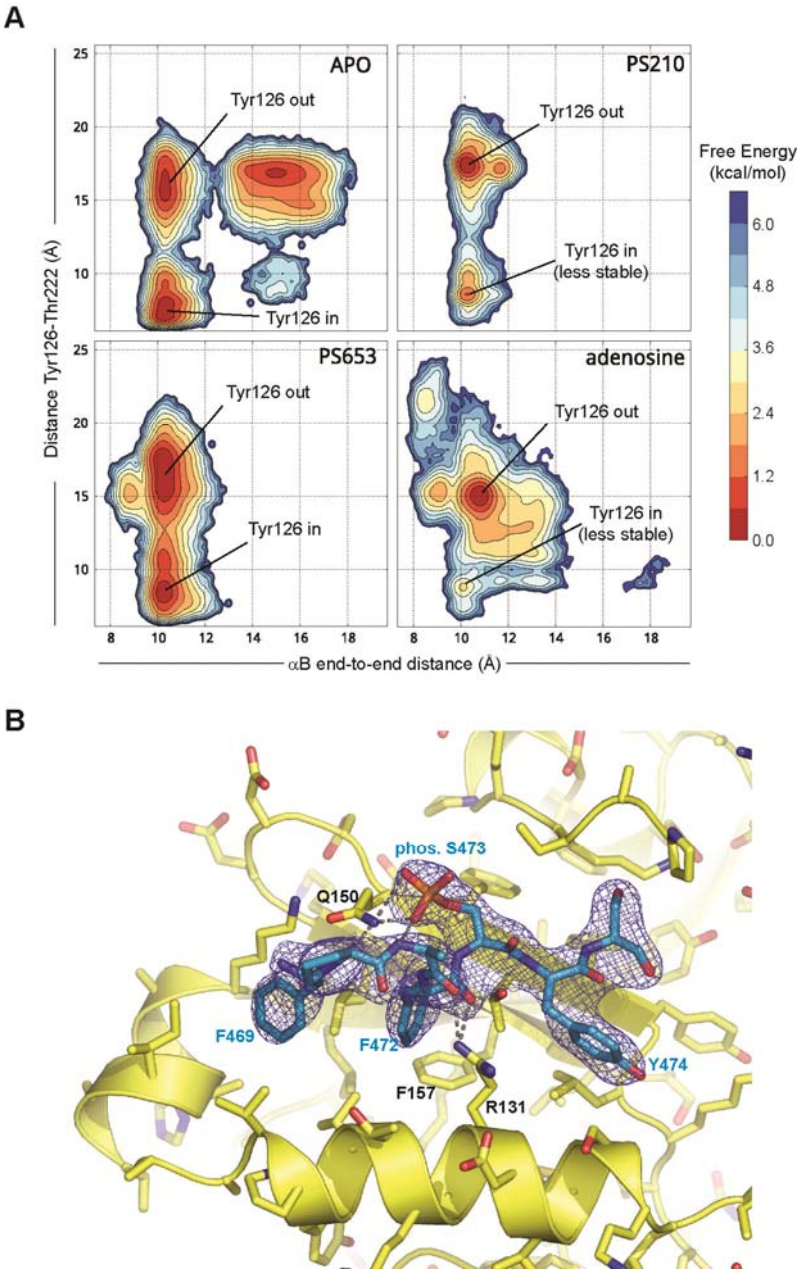

Figure S5. Related to Figure 3 and Table 1. PDK1 crystal in complex with phosphorylated HM polypeptide and MD simulations reveal new conformation of Tyr126. (**A**) Molecular dinamics of Tyr126 in the presence of ATP, PS210, PS653 and adenosine. Free energy projected along the αB end-to-end distance as in Figure 3 and figure S6 and along the distance Tyr126-Thr222, which discriminates the different orientations of Tyr126. The "alternative" conformation with the OH-group pointing towards ATP (Tyr126 "in") is less stable with PS210. (**B**) Crystal structure of PDK1 in complex with a phosphorylated HM polypeptide and ATP. The figure shows a zoom of the PIF-pocket with PDK1 (yellow) in cartoon representation and side chains as sticks. The HM polypeptide is derived from PKB/Akt and the residue numbers correspond to PKBα/Akt1. The peptide is depicted in light blue; its $|2F_o\text{-}F_c|$ electron density is shown in dark blue and contoured at 1σ. The crystal structure contains four molecules in the asymmetric unit. Residues 469-475 are well resolved in all four molecules. The structure depicts the docking interaction between the HM of substrates of PDK1 and the PIF-pocket of PDK1. This docking interaction is required for the phosphorylation of a number of substrates of PDK1, i.e. S6K and SGK, but is not required for efficient phosphorylation and activation of PKB/Akt (Biondi, et al., 2001; Busschots, et al., 2012; Collins, et al., 2003; Rettenmaier, et al., 2014). Our structure suggests that the docking interaction still takes place for Akt/PKB, even if it is not the determinant of the phosphorylation of Akt/PKB by PDK1. While writing the current manuscript, the crystal structure of PDK1 in complex with a short version of PIFtide was published (Rettenmaier, et al., 2014).

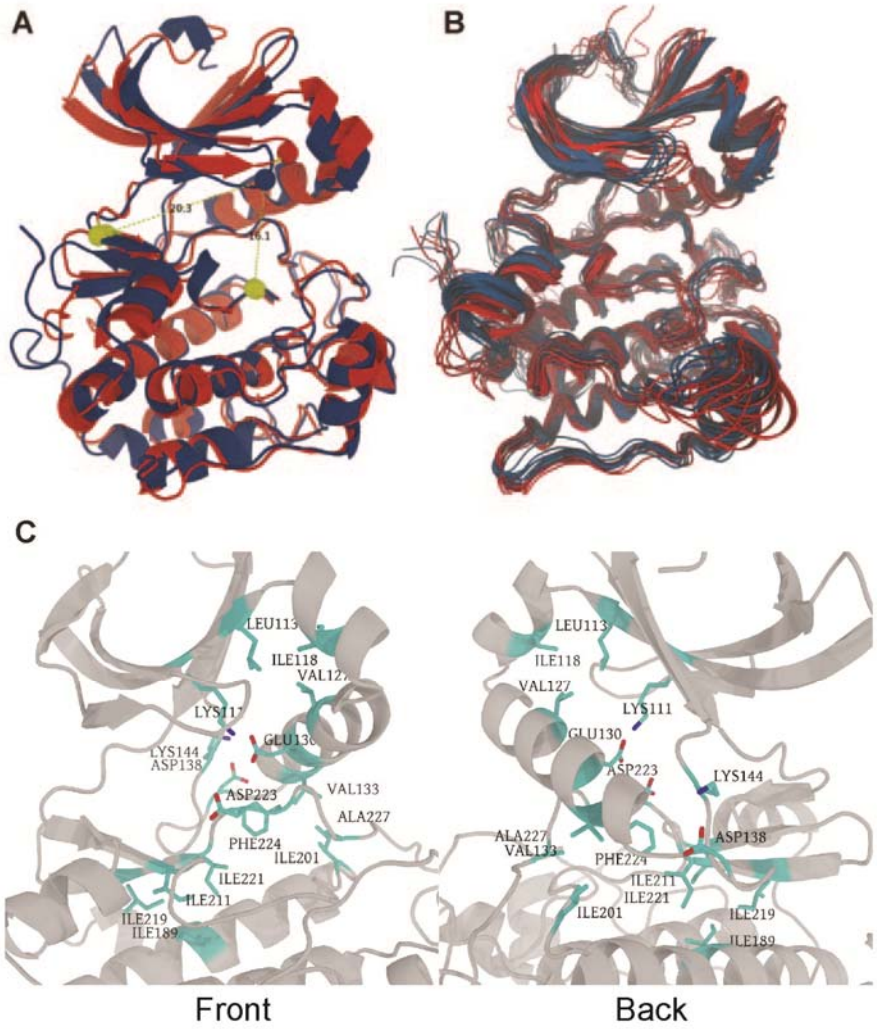

Figure S6. Related to Figure 3 and Figure 4. PT-MetaD simulations with PS210 (red) and PS653. (**A,B**) Most populated structures from the PT-MetaD simulations with PS210 (red) and PS653 (blue). While both ligands stabilize the PIF pocket, different conformations are observed, with PDK1 lobes being more twisted with PS653. (**C**) Residues that have increased interactions in the close conformation of PDK1.

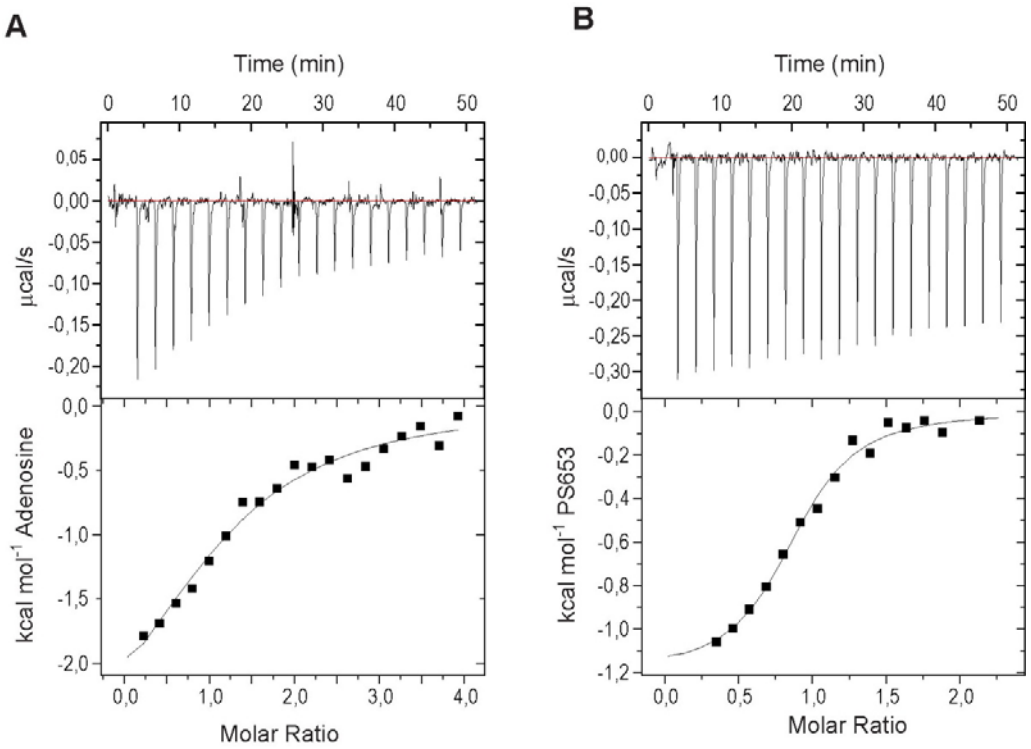

Figure S7. Related to Table 1. Characterization of adenosine and PS653 interaction with $PDK1_{50-359}$ by ITC. (**A**) Interaction of $PDK1_{50-359}$ with adenosine. (**B**) Interaction of $PDK1_{50-359}$ with PS653. The panels show the raw heat signal for successive injections of compound into a $PDK1_{50-359}$ solution. Bottom panels show the integrated heats of injections corrected for heats of dilution for compounds. The solid lines corresponding to the best fit of the data were calculated using Origin™ software. Thermodynamic parameter values are given in Table 1.

Table S1. Related to Figure 2. Crystallography: Data collection and refinement statistics. See also Figure 2; Figures S2 and S5.

	PS653	PSE10 + ATP	adenine	adenosine	phos. PBK-HM peptide + ATP
Data collection					
Space group	C2	C2	C2	C2	$P2_1$
Cell dimensions					
a, *b*, *c* (Å)	148.2, 44.4, 47.3	148.2, 44.4, 47.9	148.0, 44.4, 47.8	147.4, 44.3, 47.7	47.8, 168.5, 94.9
α, β, γ (°)	90, 100.3, 90	90, 101.8, 90	90, 102.1, 90	90, 101.4, 90	90, 93.0, 90
Resolution (Å)	73-1.4 (1.5-1.4)*	73-1.09 (1.19-1.09)	44-1.27 (1.34-1.27)	43-1.38 (1.46-1.38)	95-2.5 (2.6-2.5)
R_{sym}	5.1 (68.3) *	5.1 (68.3)	4.9 (70.7)	3.4 (55.3)	10.4 (70.8)
I / σI	14.7 (2.0) *	15.0 (2.0)	17.8 (2.4)	17.6 (2.0)	12.5 (2.2)
Completeness (%)	99.8 (99.8) *	99.7 (99.7)	99.6 (98.1)	99.0 (98.1)	99.7 (97.8)
Redundancy	4.0 (4.0) *	4.8 (3.0)	6.6 (6.2)	3.0 (3.0)	4.2 (3.8)
Refinement					
Resolution (Å)	1.4	1.09	1.27	1.38	2.5
No. reflections	59735	126722	80421	61796	51591
R_{work} / R_{free}	15.3 / 17.8	14.0 / 16.1	13.0 / 15.7	13.3 / 16.6	19.5 / 23.5
No. atoms					
Protein	2504	2371	2437	2375	9209
Ligand/ion	41	66	17	27	124
Water	267	361	310	256	324
B-factors					
Protein	21.1	14.4	22.0	21.0	50.7
Ligand/ion	27.5	26.3	23.3	28.0	60.2
Water	31.3	26.8	32.6	32.5	41.5
R.m.s deviations					
Bond lengths (Å)	0.013	0.016	0.012	0.008	0.008
Bond angles (°)	1.6	1.6	1.5	1.3	1.2

*Values in parentheses are for highest-resolution shell.

Supplemental Experimental Procedures

Supplemental Materials

Complete protease inhibitor cocktail tablets were from Roche. Protein concentration was determined using Coomassie Plus from Perbio. Protein concentration was performed using Vivaspin concentrators. Ni-NTA and Glutathione sepharose resins were from GE Healthcare. Human embryonic kidney (HEK) 293 cells (ATCC collection) were cultured in Dulbecco's modified Eagle's medium containing 10% fetal bovine serum (Gibco). Mammalian tissue culture materials were from Greiner. Insect cell expression system and all the insect cell related material were from Invitrogen. Site-directed mutagenesis was performed using a QuikChange strategy (Stratagene). DNA constructs used for transient transfection were purified from bacteria using a Qiagen plasmid Mega kit according to the manufacturer's protocol. DNA sequences were verified by automatic DNA sequencing (Applied Biosystems 3100 Genetic Analyzer).

PDK1 expression, purification and in vitro kinase assay

$PDK1_{50-359}$ employed in the crystallography work ($PDK1_{50-359}$ [Tyr288Gly; Gln292Ala]) was in addition subjected to TEV protease cleavage and re-chromatography through Ni-NTA resin before gel filtration and concentration, as described (Hindie, et al., 2009). *In vitro* PDK1 activity tests were performed using T308tide as a substrate for PDK1 essentially as previously described (Biondi, et al., 2000; Engel, et al., 2006). In brief, the PDK1 activity assay was performed at room temperature (22°C) in a 20 µl mix containing 50 mM Tris pH 7.5, 0.05 mg/ml BSA, 0.1% β-mercaptoethanol, 10 mM $MgCl_2$, 100 µM [γ^{32}P]ATP (5-50 cpm/pmol) , 0.003% Brij, 150-500 ng PDK1, and T308tide 300 µM, or 600 µM for GST-PDK1 assays). The assay was performed in a 96 well format and 4 µl aliquots spotted on p81 phosphocellulose papers (Whatmann) using ep motion 5070 (Eppendorf), washed in 0.01% phosphoric acid, dried, and then exposed and analyzed using PhosphoImager technology (FLA-9000 Starion, Fujifilm). The basal specific activities and the activity in the presence of excess of PIFtide (2 µM) of GST-PDK1 purified constructs were: GST-$PDK1_{50-359}$ [Y288G; Q292A] (wt), 0,93 U/mg, plus PIFtide 5,6 U/mg; GST-$PDK1_{50-359}$ [Tyr288GLy; Gln292Ala; Lys144Ala] (Lys144Ala), 0,65 U/mg, plus PIFtide 4,99 U/mg; GST-$PDK1_{50-359}$ [Tyr288Gly; Gln292Ala; Lys144Glu] (Lys144Glu), 0,65 U/mg, plus PIFtide 5,2 U/mg. Activity measurements were performed in duplicates or triplicates with less than 10 % difference between replicates. Activity measurements were repeated at least twice with different batches of purified proteins.

Crystal structures

We soak PDK1 crystals with the different compounds over night. However, crystals soaked at the same time with both PS653 and PS210 were completely dissolved after only 3 h. When soaked for 1 h, the crystal structure contained only PS210 (data not shown). Crystals of PDK1 in complex with the phosphorylated HM polypeptide was obtained by hanging drop vapor diffusion at 20 °C. 1.5 µl of protein solution (20 mg/ml, 4.3 mM ATP) was added to 1.5 µl of reservoir solution (1.65 M ammonium sulfate, 100 mM sodium sulate pH 5.7 and 10 mM DTT). Plate-like crystals grew to a size of 800 µm x 300 µm x 50 µm within two to three weeks.

X-ray diffraction data were collected at beamlines BL14.1 (BESSY II, HZB, Berlin) and PXIII (Swiss Light Source, Villigen). The structure of PDK1 (PDB code 3HRC(Hindie, et al., 2009)) served as a model for molecular replacement. Data were processed using the XDS program package, Phaser, PHENIX and Coot as previously performed (Busschots, et al., 2012). The following Ramachadran plot values (preferred regions/allowed regions/outliers) were obtained using Coot: PS653, 96.3/3.3/0.4; PSE10+ATP, 96.6/3.0/0.4; adenine, 98.0/2.0/0; adenosine, 96.5/3.2/0.4; HM-peptide, 94.7/5.3/0. Molecular graphic figures were prepared using PyMOL (Schrödinger).

Screening of a library of small compounds using alphascreen technology

The effects of the 14400 diverse set of small compounds (Maybridge HitFinder library; average MW 320) were tested at a concentration of 50 µM. His-PDK1 and Biotin-PIFtide in the presence of DMSO or the different compounds from the library were incubated in the dark for 90 min at room temperature and the emission of light from the acceptor beads was measured in the EnVision reader (Perkin Elmer). The identified hits were compared with those identified in an equivalent screening using His-Aurora kinase and biotin-TPX2. The hits that specifically affected the PDK1-PIFtide screening were further investigated for validation. PS653 (Maybridge code RH00237) and PSE10 (Maybridge code RF02011) are representatives of different validated hits identified that

displaced the PDK1-PIFtide interaction. The interaction between GST-PDK1$_{50-359}$ [Tyr288Gly; Gln292Ala] (wt) and biotin-PIFtide was measured in the same assay but using anti-GST and streptavidin-coated donor beads. The conditions for all alphascreen asays were identified in a cross-titration experiment by varying the concentrations of PDK1 and biotin-PIFtide. Conditions were chosen to have 50000-100000 alphascreen counts and be in a linear range. All GST-PDK1 assays contained 1.6 nM PDK1; the interaction with PDK1 wt was measured in the presence of 6.25 nM biotin-PIFtide; 25 nM and 100 nM biotin-PIFtide were used to measure the effect of compounds on GST-PDK1$_{50-359}$ [Tyr288Gly; Gln292Ala; Lys144Ala] (Lys144Ala) and PDK1$_{50-359}$ [Tyr288Gly; Gln292Ala; Lys144Glu] (Lys144Glu), respectively. When the assay was performed with GST-PDK1 constructs, the displacement of biotin-PIFtide by PS653 reached 50%. Except for the original screening, the assays were performed at least twice, in duplicates and with proteins from at least two different purifications. Representative experiments are shown.

Details of molecular dynamics simulations

The system was minimized with 10000 steps of conjugated gradient and equilibrated in the NPT ensemble for 10 ns. A production run of 400 ns was then performed in the NVT ensemble, with a time step of 2 fs. Neighbor searching was performed every 5 steps. The PME algorithm was used for electrostatic interactions with a cut-off of 1.2 nm, while a single cut-off of 1.2 nm was used for Van der Waals interactions. Temperature coupling was done with the V-rescale algorithm (Bussi, et al., 2007).

Isothermal titration calorimetry

Titrations were performed by a 0.4 µl injection followed by 19 successive injections (2 µl) of each compound (adenosine 500 µM, PS653 250 µM) into a 202 µl reaction cell containing PDK1$_{50-359}$ (26.5 µM and 23 µM, respectively). For the titrations of PDK1 with adenosine, the protein and the compound were prepared in 50 mM Tris-HCl (pH 7.4), 200 mM NaCl, 1 mM DTT and 1% v/v DMSO. For the titration of PDK1 with PS653 the protein and the compound were prepared in 50 mM Tris-HCl (pH 7.4), 200 mM NaCl, 1 mM DTT and 5% v/v DMSO. Errors on the thermodynamic parameter values in Table 1 are non linear least square fitting errors of the experimental binding isotherms using the Levenberg-Markardt iteration method (Freire et al., 2009). The titration of PDK1 with adenosine was performed at 25ºC, and the titration of PDK1 with PS653 was made at 37ºC. Raw calorimetric data were corrected for heats of dilution. Binding stoichiometries, enthalpy values and K_d values were determined by fitting corrected data to a model with one type of sites using Origin7 software (MicroCal Inc.).

Small molecules PSE10 and PS653

All ^{1}H-NMR and ^{13}C-NMR spectra were measured on AMX 400 (400MHz) spectrometers. Chemical shifts (δ) are reported in parts per million (ppm). For peak multiplicity are used: s, singlet; d, doublet; t, triplet; m, multiplet. J values are given in Hz. ESI mass spectra were recorded on a Fisons VG Plattform II spectrometer.

PSE10 ('2-oxopropyl N-(4-chlorophenyl)- [(2-chloro-6-fluorobenzoyl)amino] methanimidothioate; Maybridge RF02011). $C_{17}H_{13}Cl_2FN_2O_2S$ [399. 26 g/mol]. ^{1}H-NMR (400 MHz, DMSO-d_6) [δ ppm]: 7.52 (m, 2H), 7.38 (m, 1H), 7.31 (m, 3H), 7.19 (m, 1H), 7.03 (s, 1H), 3.64 (m, 1H), 3.41 (m, 1H), 1.40 (s, 3H). ^{13}C-NMR (100 MHz, DMSO-d_6) [δ ppm]: 173.08, 172.36, 159.64, 157.17, 136.21, 132.82, 131.28, 130.93, 130.61, 130.52, 130.37, 130.30, 128.79, 128.29, 125.40, 125.36, 114.72, 114.50, 91.78, 25.83. ESI-MS (M+H$^+$): 399.00.

PS653 ('1,6-dihydrodibenzo[cd, g]indazol-6-one; Maybridge RH00237). $C_{14}H_8N_2O$ [220.23 g/mol]. ^{1}H-NMR (400 MHz, DMSO-d_6) [δ ppm]: 13.70 (bs, 1H, NH), 8.32 (d, J= 8.06Hz, 1H), 8.23 (d, J= 8.06Hz, 1H), 8.02 (d, J= 8.22Hz,1H), 7.96 (d, J= 7.15Hz,1H), 7.82 (t, J= 7.45Hz, 1H), 7.74 (m, 1H), 7.61 (t, J= 7.45 Hz, 1H). ^{13}C-NMR (100 MHz, DMSO-d_6) [δ ppm]: 182.79, 139.13, 138.28, 133.66, 132.62, 131.64, 128.57, 128.52, 128.36, 125.17, 122.41, 122.10, 120.18, 117.02. ESI-MS (M+H$^+$): 221.07.

References

Bayascas, J.R. (2008). Dissecting the role of the 3-phosphoinositide-dependent protein kinase-1 (PDK1) signalling pathways. Cell Cycle 7, 2978-2982.

Biondi, R.M., Cheung, P.C., Casamayor, A., Deak, M., Currie, R.A., and Alessi, D.R. (2000). Identification of a pocket in the PDK1 kinase domain that interacts with PIF and the C-terminal residues of PKA. Embo J 19, 979-988.

Biondi, R.M., Kieloch, A., Currie, R.A., Deak, M., and Alessi, D.R. (2001). The PIF-binding pocket in PDK1 is essential for activation of S6K and SGK, but not PKB. Embo J 20, 4380-4390.

Busschots, K., Lopez-Garcia, L.A., Lammi, C., Stroba, A., Zeuzem, S., Piiper, A., Alzari, P.M., Neimanis, S., Arencibia, J.M., Engel, M., et al. (2012). Substrate-Selective Inhibition of Protein Kinase PDK1 by Small Compounds that Bind to the PIF-Pocket Allosteric Docking Site. Chem Biol 19, 1152-1163.

Bussi, G., Donadio, D., and Parrinello, M. (2007). Canonical sampling through velocity rescaling. J Chem Phys 126, 014101.

Collins, B.J., Deak, M., Arthur, J.S., Armit, L.J., and Alessi, D.R. (2003). In vivo role of the PIF-binding docking site of PDK1 defined by knock-in mutation. Embo J 22, 4202-4211.

Engel, M., Hindie, V., Lopez-Garcia, L.A., Stroba, A., Schaeffer, F., Adrian, I., Imig, J., Idrissova, L., Nastainczyk, W., Zeuzem, S., et al. (2006). Allosteric activation of the protein kinase PDK1 with low molecular weight compounds. Embo J 25, 5469-5480.

Frodin, M., Antal, T.L., Dummler, B.A., Jensen, C.J., Deak, M., Gammeltoft, S., and Biondi, R.M. (2002). A phosphoserine/threonine-binding pocket in AGC kinases and PDK1 mediates activation by hydrophobic motif phosphorylation. Embo J 21, 5396-5407.

Hindie, V., Stroba, A., Zhang, H., Lopez-Garcia, L.A., Idrissova, L., Zeuzem, S., Hirschberg, D., Schaeffer, F., Jorgensen, T.J.D., Engel, M., et al. (2009). Structure and allosteric effects of low molecular weight activators on the protein kinase PDK1. Nat. Chem. Biol. 5, 758-764.

Rettenmaier, T.J., Sadowsky, J.D., Thomsen, N.D., Chen, S.C., Doak, A.K., Arkin, M.R., and Wells, J.A. (2014). A small-molecule mimic of a peptide docking motif inhibits the protein kinase PDK1. Proc Natl Acad Sci U S A 111, 18590-18595.

Yang, J., Cron, P., Thompson, V., Good, V.M., Hess, D., Hemmings, B.A., and Barford, D. (2002). Molecular mechanism for the regulation of protein kinase B/Akt by hydrophobic motif phosphorylation. Mol Cell 9, 1227-1240.

Zheng, J., Knighton, D.R., ten Eyck, L.F., Karlsson, R., Xuong, N., Taylor, S.S., and Sowadski, J.M. (1993). Crystal structure of the catalytic subunit of cAMP-dependent protein kinase complexed with MgATP and peptide inhibitor. Biochemistry 32, 2154-2161.